SMEDWI-2 Is a PIWI-Like Protein That Regulates Planarian Stem Cells

Peter W. Reddien,* Néstor J. Oviedo,† Joya R. Jennings, James C. Jenkin, Alejandro Sánchez Alvarado‡

We have identified two genes, *smedwi-1* and *smedwi-2*, expressed in the dividing adult stem cells (neoblasts) of the planarian *Schmidtea mediterranea*. Both genes encode proteins that belong to the Argonaute/PIWI protein family and that share highest homology with those proteins defined by *Drosophila* PIWI. RNA interference (RNAi) of *smedwi-2* blocks regeneration, even though neoblasts are present, irradiation-sensitive, and capable of proliferating in response to wounding; *smedwi-2(RNAi)* neoblast progeny migrate to sites of cell turnover but, unlike normal cells, fail at replacing aged tissue. We suggest that SMEDWI-2 functions within dividing neoblasts to support the generation of cells that promote regeneration and homeostasis.

Members of the PIWI/Argonaute family of proteins fall into two main classes, one named after *Arabidopsis* Argonaute and the other after *Drosophila* PIWI (*1*). Members of this protein family contain PAZ and PIWI domains and mediate silencing via cleavage of mRNAs (*2*–*4*) or by inhibition of translation (*5*, *6*). These proteins are found in plants (*7*), yeast (*8*), and throughout the animal kingdom—including at least eight in humans. Some of the PIWI-class proteins have been implicated in the regulation of germ cells (*9*–*11*). Very little is known, however, about how PIWI proteins regulate germ cells and whether these proteins typically promote stem cell maintenance or differentiation. Furthermore, the types of stem cells and developmental events regulated by PIWI-class proteins remain unclear.

Here we report on the planarian *S. mediterranea* genes *smedwi-1* and *smedwi-2*. We studied *smedwi-1* and *-2* because they encode proteins similar to the PIWI class of PIWI/Argonaute proteins (fig. S1) and are thus candidates to regulate the adult somatic stem cells (neoblasts) of planarians (*12*, *13*). Furthermore, *smedwi-1* expression resembles the distribution of planarian neoblasts (*14*). Planarians present a promising venue for the study of PIWI-like genes because stem cells play prominent roles in homeostasis and regeneration and because the genetic study of planarian stem cells is now possible (*12*, *13*, *15*).

smedwi-1 and *smedwi-2* are expressed in small cells distributed like neoblasts—that is, posterior to photoreceptors and excluded from the pharynx (Fig. 1, A to C). *smedwi*-expressing cells, like neoblasts, reside in the parenchyma: mesenchymal tissue excluded from the nervous system, pharynx, and gastrovascular system (Fig. 1, D and E). Neoblasts are quickly and specifically eliminated after irradiation (*12*). Expression of *smedwi-1* and

Howard Hughes Medical Institute, Department of Neurobiology and Anatomy, University of Utah School of Medicine, Salt Lake City, UT 84132, USA.

*Present address: MIT Biology, Whitehead Institute, Cambridge, MA 02142, USA.
†Present address: Cytokine Biology Department, Forsyth Institute, Harvard Medical School, Boston, MA 02115, USA.
‡To whom correspondence should be addressed. E-mail: sanchez@neuro.utah.edu

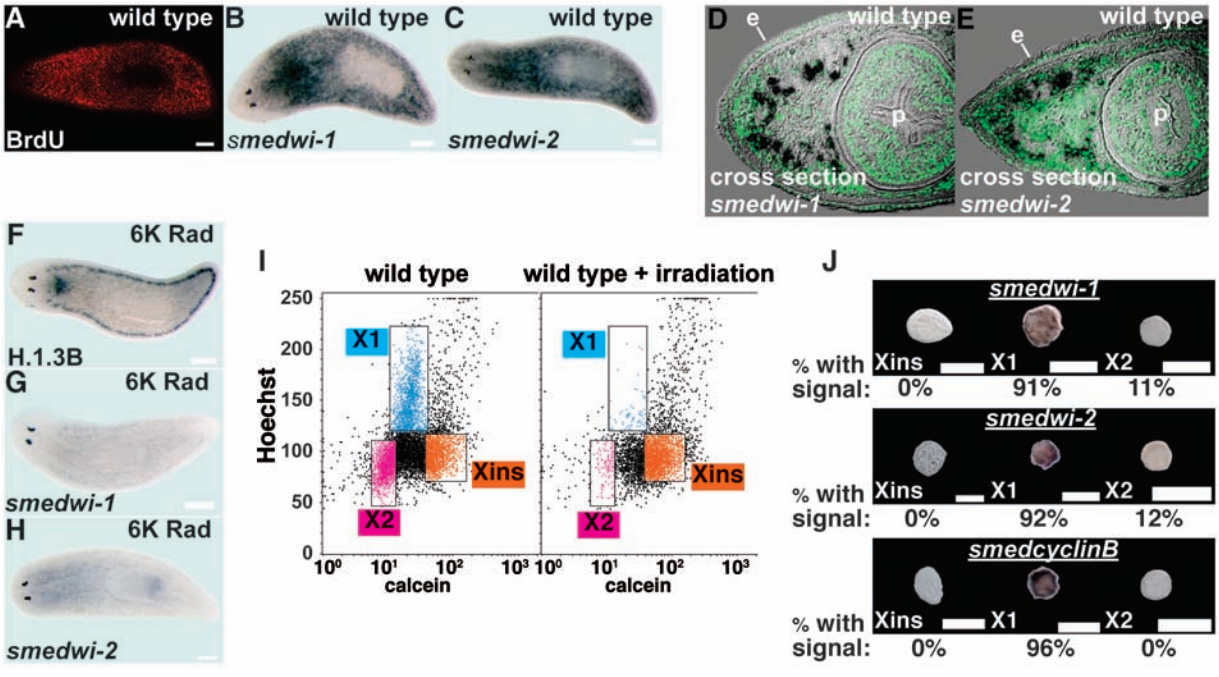

Fig. 1. Dividing neoblasts express *smedwi-1* and *smedwi-2*. (**A**) BrdU labeling demonstrates neoblast distribution; (**B** and **C**) *smedwi-1* and *-2* expression resembles neoblast distribution. Riboprobes are identified at lower left; anterior is to the left. (**D** and **E**) Tissue cross sections, dorsal up. Green, nuclei; black, *smedwi* expression; e, epidermis; p, pharynx. (**F** to **H**) Irradiation at 6000 rad. After irradiation, *smedwi-1* signals (4/4 at 48 hours, 5/5 at 72 hours) and *smedwi-2* signals (2/2 at 48 hours, 8/8 at 72 hours) were undetectable. H.1.3B is an irradiation-insensitive control. (**I**) FACS profile of *S. mediterranea* cells (≤20 μm), Hoechst- and calcein-labeled. X1 (blue) and X2 (pink) populations are irradiation-sensitive; Xins (orange) population is not. (**J**) *smedwi-1* (top), *smedwi-2* (middle), and *smedcyclinB* [clone NBE.6.09E (AY967658); bottom] in situ hybridizations on FACS-isolated cells. Representative results are shown. Expression was typically in X1 but not X2 or Xins cells. Percentages are signal-positive cells ($n > 210$ cells each). Scale bars, 0.2 mm [(A) to (C), (F) to (H)], 10 μm (J).

-2 was markedly reduced by irradiation, consistent with their possible expression in neoblasts (Fig. 1, F to H) (table S1).

Flow cytometry has been used to separate planarian cells and identify neoblasts (*16*, *17*). We used flow cytometry to isolate two populations of irradiation-sensitive cells with neoblast morphology, named X1 and X2, and examined *smedwi-2* expression (Fig. 1I). In situ hybridizations and quantitative reverse transcription polymerase chain reactions indicated that *smedwi* genes are predominantly expressed within X1 cells, at low percentages in X2 cells, and perhaps absent from control irradiation-insensitive Xins cells (Fig. 1J) (table S2). Because neoblasts proliferate, we asked whether cell cycle differences between X1 and X2 cells exist by examining expression of an *S. mediterranea* gene homologous to the cell division marker *cyclinB* (*smedcyclinB*). We observed *smedcyclinB* expression in 96% of X1 cells (n = 325) and 0% of X2 cells (n = 257) (Fig. 1J), which suggests that X1 cells are dividing. Together, our data indicate that *smedwi* genes are expressed directly and largely specifically within dividing neoblasts.

To investigate how SMEDWI proteins regulate neoblasts, we inhibited *smedwi-1* and *-2* with the use of RNA interference (RNAi). RNAi affected expression specifically (fig. S2A). RNAi of *smedwi-1* did not cause robust defects, but RNAi of *smedwi-2* resulted in 100% penetrant defects resembling those in irradiated animals lacking neoblasts. Irradiated and *smedwi-2(RNAi)* animals displayed regression of tissue anterior to the photoreceptors, were incapable of regeneration, and curled around their ventral surface (Fig. 2, A to C). Head regression likely occurred because tissue in front of the photoreceptors lacks dividing neoblasts and is constantly replaced by neoblast progeny (*12*). Because *smedwi-2(RNAi)* animals resemble irradiated animals, *smedwi-2* is likely needed for neoblast function.

smedwi-2(RNAi) defects progress through temporal stages, ending in lethality (fig. S2B). At ≥8 days after exposure to *smedwi-2* double-stranded RNA (dsRNA), animals were incapable of regeneration. Animals wounded earlier could regenerate small blastemas that regressed (fig. S2C). Homeostasis defects after *smedwi-2* silencing arose with kinetics similar to those in irradiated animals. For example, 9 days after irradiation, 15 of 30 animals displayed head regression, whereas 9 days after *smedwi-2* dsRNA feeding, 12 of 29 animals did so. Because irradiation prevents new cell production within 24 hours, homeostasis is likely disrupted within a day after *smedwi-2* inhibition (fig. S2B). SMEDWI-2 protein levels sufficient for neoblast function in tissue turnover likely do not perdure after RNAi. This hypothesis is supported by the observation that *smedwi-2* is expressed in dividing cells, which

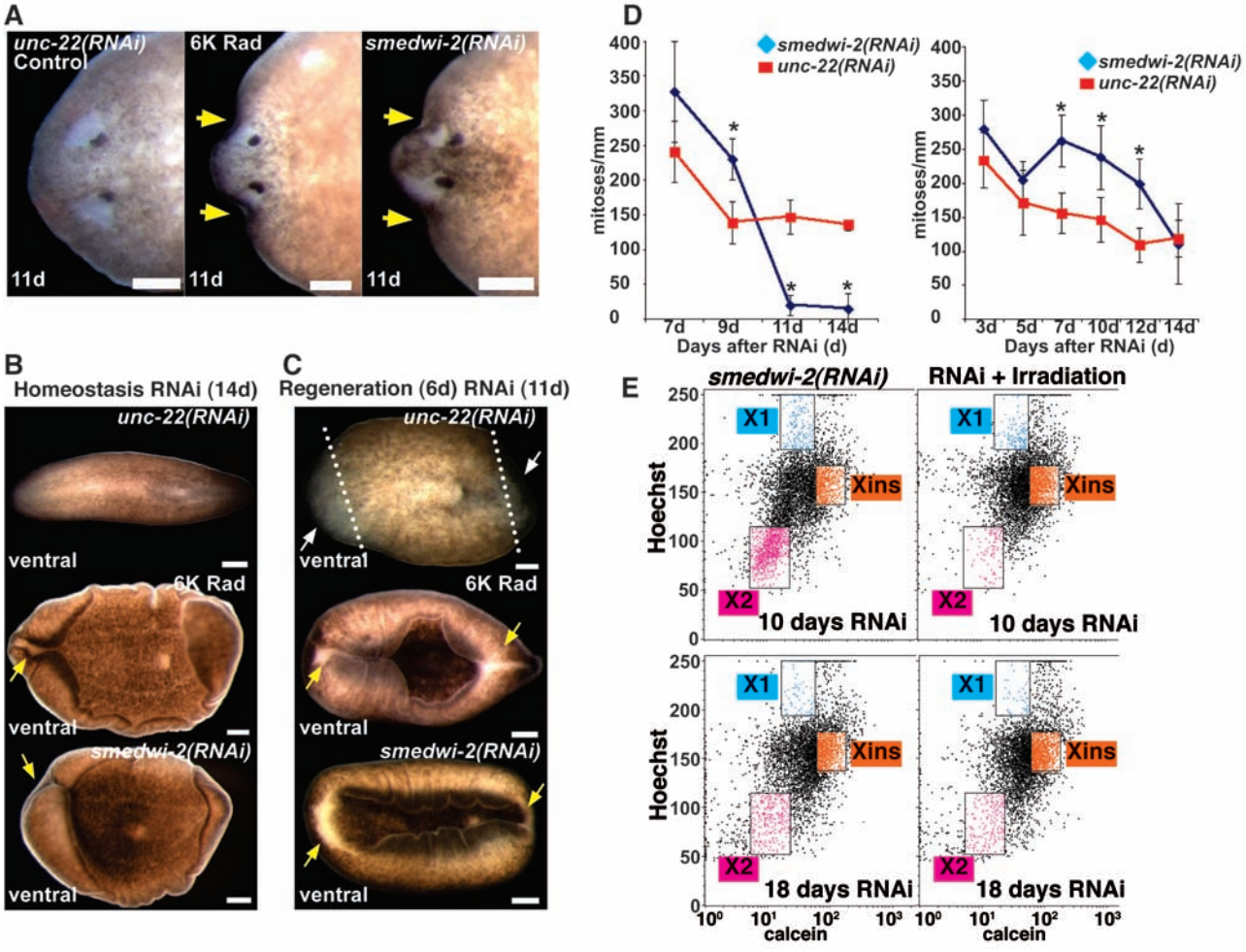

Fig. 2. *smedwi-2(RNAi)* animals display defects related to neoblast dysfunction. (**A** to **C**) Irradiation at 6000 rad. *C. elegans unc-22*, negative control. Anterior is to the left; scale bar, 0.2 mm. Yellow arrowheads show head regression. In (B) and (C); ventral is up; in (C), heads and tails are amputated [dotted line, blastema (unpigmented) boundary]. White arrows, blastemas; yellow arrows, healed wounds without blastema. (**D**) Mitotic numbers divided by animal length. Left panel: Two dsRNA feedings, ≥5 animals per time point. Times shown are days after first feeding. Right panel: One dsRNA feeding, ≥6 animals per time point. Control numbers decline with time because feedings boost mitotic numbers. *P < 0.001, t test. (**E**) Cell numbers were analyzed by FACS (see Fig. 1I for nomenclature). Control irradiations were done 5 days before analysis. *smedwi-2(RNAi)* X1 and X2 irradiation-sensitive populations were present 10 days after RNAi but were greatly reduced by 18 days.

indicates that new protein is produced with new cell production.

One simple explanation for the *smedwi-2(RNAi)* phenotype would be absence of neoblasts. Neoblasts are the only known mitotic cells in adult planarians (*12*). We observed that mitotic numbers in *smedwi-2(RNAi)* animals always eventually plummet (Fig. 2D). We quantified this defect in intact RNAi animals. As expected, at days 11 and 14, *smedwi-2(RNAi)* animals had far fewer mitotic cells than did controls ($P < 0.001$, *t* test). However, *smedwi-2(RNAi)* animals at day 9 were defective for regeneration but had greater mitotic numbers than did the control ($P < 0.001$). We designed a second time course to carefully observe this increase (Fig. 2D). Because feeding boosts mitotic numbers, a single feeding was used so that early time points could be more easily observed. A clear and significant increase in mitotic numbers above the control was observed at days 7, 10, and 12 in *smedwi-2(RNAi)* animals ($P < 0.001$). In situ hybridizations with the *smedwi-1* riboprobe indicated that X1 cells sharply decline in numbers rather than lose the capacity to divide at late time points after RNAi (fig. S2D). Fluorescence-activated cell sorting (FACS) analyses indicated that both X1 and X2 cells were present and irradiation-sensitive in *smedwi-2(RNAi)* animals incapable of regeneration 10 and 12 days after RNAi but were greatly diminished by days 14 through 18 (Fig. 2E) (fig. S3).

These experiments revealed several important aspects of the *smedwi-2* phenotype. First, and in contrast to irradiated animals, neoblasts were present and proliferating at times after RNAi when animals could not regenerate. This suggests that failed neoblast maintenance was not the primary cause of failed regeneration and tissue turnover. Second, at early time points after RNAi, a greater number of *smedwi-2(RNAi)* mitotic neoblasts were present than in controls, suggesting a feedback regulation from loss of tissue homeostasis. Because tissue turnover fails quickly after RNAi of *smedwi-2*, mitotic numbers may increase during this period as a consequence of failed homeostasis. Finally, in late phases of the *smedwi-2* phenotype, neoblasts are not maintained. Long-term neoblast maintenance abnormalities could be a secondary result of failed homeostasis.

We asked whether *smedwi-2(RNAi)* neoblasts were capable of responding to wounds in animals incapable of regeneration. Specifically, we quantified mitotic numbers in prepharyngeal animal fragments that were or were not proximal to a wound produced 14 hours earlier (Fig. 3A). We determined that *smedwi-2(RNAi)* animals were capable of mounting an apparently normal proliferative wounding response (Fig. 3A, $P < 0.001$). This finding indicates that the primary defect that blocked blastema formation in *smedwi-2(RNAi)* animals was not a gross dysfunction in the ability of neoblasts to detect wounds. We therefore propose that neoblast progeny function (e.g., differentiation, migration) is the primary abnormality underlying the *smedwi-2(RNAi)* phenotype.

To assess whether neoblast progeny can migrate, we labeled them with 5-bromo-2′-deoxyuridine (BrdU) and examined head tips, a region devoid of proliferating cells and into which labeled cells migrate (*18*). The progeny of *smedwi-2(RNAi)* neoblasts did not grossly fail to migrate in front of the photoreceptors of regressing heads (Fig. 3B); this result suggests that *smedwi-2(RNAi)*

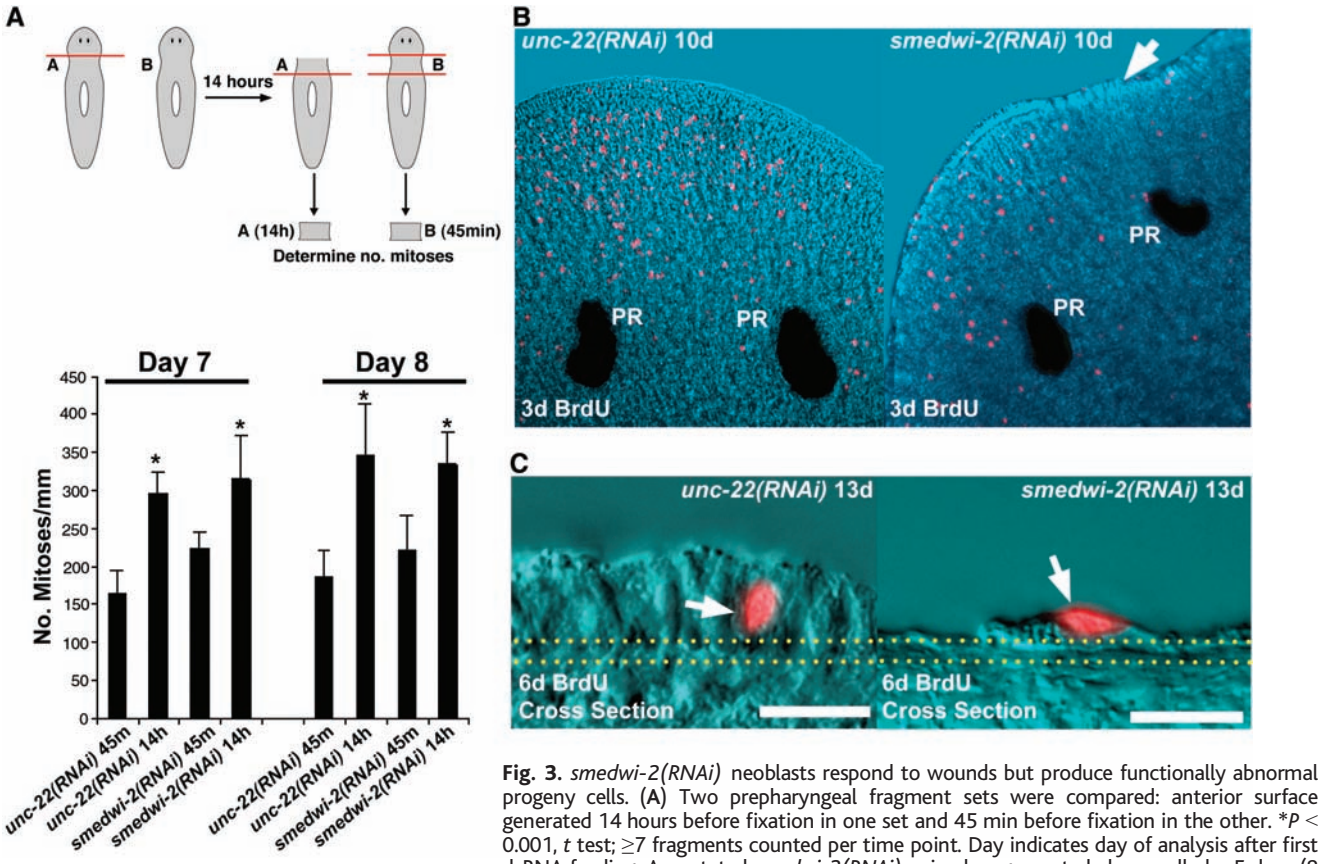

Fig. 3. *smedwi-2(RNAi)* neoblasts respond to wounds but produce functionally abnormal progeny cells. (**A**) Two prepharyngeal fragment sets were compared: anterior surface generated 14 hours before fixation in one set and 45 min before fixation in the other. *$P <$ 0.001, *t* test; ≥7 fragments counted per time point. Day indicates day of analysis after first dsRNA feeding. Amputated *smedwi-2(RNAi)* animals regenerated abnormally by 5 days (8 of 22 animals amputated on day 7 had very small blastemas and 14 of 22 had no blastemas; 8 of 30 animals amputated on day 8 had very small blastemas and 22 of 30 had no blastemas). All controls were normal (day 7, $n = 26$; day 8, $n = 20$). (**B**) Cells in red are BrdU-positive 3 days after labeling. White arrowhead, tissue regression 10 days after dsRNA exposure; PR, photoreceptors. Proliferative neoblasts do not exist anterior to photoreceptors, which indicates that neoblast progeny migrated. Anterior is up; scale bar, 0.1 mm. (**C**) Postpharyngeal cross sections 13 days after RNAi and 6 days after BrdU labeling. White arrows, BrdU-positive cells in epidermis (outermost cells). Dotted lines are on both sides of the basement membrane of the single-cell epidermal layer. Ventral surface is up; scale bar, 10 μm.

neoblasts produced cells capable of reaching sites of tissue turnover.

Next, we asked whether neoblast progeny were capable of producing differentiated cells. Neoblast progeny normally begin to replace aged epidermal cells within a week after labeling (*18*). We sectioned BrdU-labeled *smedwi-2(RNAi)* animals after BrdU incorporation and determined that labeled cells entered the epidermis sooner than in the control and displayed a grossly abnormal morphology (Fig. 3C) (fig. S4 and table S3). Planarian epidermal cells reside in a single-cell layer and display classic columnar epithelial morphology. BrdU-labeled *smedwi-2(RNAi)* cells that reach the epidermis, however, fail to adopt a columnar morphology. For example, the average heights of BrdU-labeled epidermal cells were significantly different in *smedwi-2(RNAi)* animals and control *unc-22(RNAi)* animals: 3.5 ± 1.6 μm (n = 18) and 10.0 ± 1.9 μm (n = 10), respectively ($P < 0.0001$, t test). Regions posterior to the photoreceptors, where epidermis could be clearly visualized, were observed. In *smedwi-2(RNAi)* animals, heads regress and the cells that reach the epidermis in the body are morphologically abnormal; for this reason, we suggest that neoblast progeny cells migrate to sites of tissue turnover but fail to function normally. That the defect is within neoblast progeny is supported by the observations that *smedwi-2(RNAi)* animals resemble irradiated animals and that *smedwi-2* is expressed in the neoblasts.

How might a primary defect in *smedwi-2(RNAi)* neoblast progeny relate to the secondary defect in neoblast maintenance? Although it is unknown how an aging differentiated cell population affects neoblast division patterns, one possibility is that neoblasts are depleted because of their failure to quench an ever-increasing demand for differentiated cell replacement.

Our results provide mechanistic insight into how specific cellular events of planarian regeneration are controlled. PIWI-like proteins regulate molecular processes involving small RNAs; SMEDWI-2 may regulate some aspect of RNA metabolism within dividing neoblasts. Our data suggest that SMEDWI-2 is not needed primarily for neoblast maintenance, but rather for the production of neoblast progeny capable of replacing aged differentiated cells during homeostasis and missing tissues during regeneration. Consistent with this suggestion, the mouse PIWI-related proteins MIWI and MILI are needed for the completion of spermatogenesis but not for primordial germ cell formation (*10*, *11*). Because human *hiwi* is expressed in primitive hematopoietic cells, PIWI proteins may regulate multiple types of stem cells (*19*). We suggest that PIWI proteins may be universal regulators of the production of stem cell progeny competent for performing differentiated functions.

References and Notes

1. M. A. Carmell, Z. Xuan, M. Q. Zhang, G. J. Hannon, *Genes Dev.* **16**, 2733 (2002).
2. G. Meister *et al.*, *Mol. Cell* **15**, 185 (2004).
3. J. Liu *et al.*, *Science* **305**, 1437 (2004).
4. T. A. Rand, K. Ginalski, N. V. Grishin, X. Wang, *Proc. Natl. Acad. Sci. U.S.A.* **101**, 14385 (2004).
5. K. Okamura, A. Ishizuka, H. Siomi, M. C. Siomi, *Genes Dev.* **18**, 1655 (2004).
6. R. S. Pillai, C. G. Artus, W. Filipowicz, *RNA* **10**, 1518 (2004).
7. K. Bohmert *et al.*, *EMBO J.* **17**, 170 (1998).
8. A. Sigova, N. Rhind, P. D. Zamore, *Genes Dev.* **18**, 2359 (2004).
9. D. N. Cox *et al.*, *Genes Dev.* **12**, 3715 (1998).
10. S. Kuramochi-Miyagawa *et al.*, *Development* **131**, 839 (2004).
11. W. Deng, H. Lin, *Dev. Cell* **2**, 819 (2002).
12. P. W. Reddien, A. Sánchez Alvarado, *Annu. Rev. Cell Dev. Biol.* **20**, 725 (2004).
13. P. W. Reddien, A. L. Bermange, K. J. Murfitt, J. R. Jennings, A. Sánchez Alvarado, *Dev. Cell* **8**, 635 (2005).
14. A. Sánchez Alvarado, P. A. Newmark, S. M. Robb, R. Juste, *Development* **129**, 5659 (2002).
15. P. A. Newmark, A. Sánchez Alvarado, *Nat. Rev. Genet.* **3**, 210 (2002).
16. M. Asami *et al.*, *Zool. Sci.* **19**, 1257 (2002).
17. K. Ogawa *et al.*, *Dev. Growth Differ.* **44**, 191 (2002).
18. P. Newmark, A. Sánchez Alvarado, *Dev. Biol.* **220**, 142 (2000).
19. A. K. Sharma *et al.*, *Blood* **97**, 426 (2001).

20. We thank K. Agata for FACS protocols, N. H. Oh for FACS assistance, P. Newmark and F. Cebriá for discussions, B. Pearson for comments, and all Sánchez lab members for support. P.W.R. is a Helen Hay Whitney Foundation fellow. A.S.A. is a Howard Hughes Medical Institute Investigator. Supported by National Institute of General Medical Sciences grant RO-1 GM57260 (A.S.A.).

Supporting Online Material

www.sciencemag.org/cgi/content/full/310/5752/1327/DC1
Materials and Methods
Figs. S1 to S4
Tables S1 to S3
References

14 June 2005; accepted 26 October 2005
10.1126/science.1116110

LIN-12/Notch Activation Leads to MicroRNA-Mediated Down-Regulation of Vav in *C. elegans*

Andrew S. Yoo[1] and Iva Greenwald[2]*

Cell-cell interactions and cross-talk between signaling pathways specify *Caenorhabditis elegans* vulval precursor cells (VPCs) to adopt a spatial pattern: a central "1°" VPC, in which epidermal growth factor receptor (EGFR)–mitogen-activated protein kinase (MAPK) activity is high and LIN-12/Notch activity is low, flanked by two "2°" VPCs, in which LIN-12/Notch activity is high and EGFR-MAPK activity is low. Here, we identify a microRNA gene, *mir-61*, as a direct transcriptional target of LIN-12 and show that expression of *mir-61* promotes the 2° fate. We also identify *vav-1*, the ortholog of the Vav oncogene, as a target of *mir-61*, and show that down-regulation of VAV-1 promotes *lin-12* activity in specifying the 2° fate. Our results suggest that *lin-12*, *mir-61*, and *vav-1* form a feedback loop that helps maximize *lin-12* activity in the presumptive 2° VPCs.

Six multipotential VPCs, numbered P3.p to P8.p, adopt an invariant pattern of fates termed 3°-3°-2°-1°-2°-3° (Fig. 1A). Two signaling events specify this pattern: "inductive" signaling, mediated by an EGFR-Ras-MAPK pathway, and "lateral" signaling, mediated by LIN-12 (Fig. 1A) (*1*). The inductive signal from the gonad activates an EGFR-Ras-MAPK cascade in a graded fashion in the underlying VPCs, P5.p, P6.p, and P7.p. The centralmost VPC, P6.p, has the highest level of EGFR-Ras-MAPK activation and becomes the presumptive 1° VPC; it produces the lateral signal, which activates LIN-12 in P5.p and P7.p. When LIN-12 is activated, proteolysis releases its intracellular domain, which translocates to the nucleus and forms a transcriptional activation complex with the DNA binding protein LAG-1 (*2*). Transcriptional targets of LIN-12 in P5.p and P7.p can be identified by the presence of LAG-1 binding sites (LBSs) in their 5′ flanking regions and include genes that encode negative regulators of EGFR-Ras-MAPK activity in P5.p and P7.p, which inhibit the expression of 1° fate features in these cells (*3*).

Short regulatory microRNAs (miRNAs), first identified in *C. elegans* (*4*), mediate post-transcriptional down-regulation of target genes. The profound and pervasive roles that miRNAs play as critical regulators of developmental gene expression are only now becoming fully appreciated. We obtained an indication that a

[1]Integrated Program in Cellular, Molecular, and Biophysical Studies, [2]Department of Biochemistry and Molecular Biophysics, Howard Hughes Medical Institute, Columbia University College of Physicians and Surgeons, 701 West 168th Street, Room 720, New York, NY 10032, USA.

*To whom correspondence should be addressed. E-mail: greenwald@cancercenter.columbia.edu

www.sciencemag.org/cgi/content/full/310/5752/1327/DC1

Supporting Online Material for

SMEDWI-2 Is a PIWI-like Protein that Regulates Planarian Stem Cells

Peter W. Reddien, Néstor J. Oviedo, Joya R. Jennings, James C. Jenkin, Alejandro Sánchez Alvarado*

*To whom correspondence should be addressed. E-mail: sanchez@neuro.utah.edu

Published 25 November 2005, *Science* **310**, 1327 (2005)
DOI: 10.1126/science.1116110

This PDF file includes:

Supporting Online Material

Materials and Methods

GeneBank accession numbers for *smedwi-1* and *smedwi-2* are DQ186985 and DQ186986.

In situ hybridizations

Animals were fixed in Carnoy's fixative as described previously and stored in methanol. Following re-hydration with a methanol:PBST (PBS, 0.1% triton X-100) dilution series, animals were incubated at 56°C for 2 hours in pre-hybridization solution (50% formamide, 5X SSC pH 7.0, 100µg/mL heparin, 0.05% tween-20, 0.05% triton X-100, 5mM DTT, 1mg/mL yeast RNA, 1X Denhardt's). Hybridization with digoxigenin (DIG)-conjugated riboprobes was done for 16 hours in hybridization solution (same as pre-hybridization solution, except plus 5% dextran sulfate). Animals were washed with wash Hybe (50% formamide, 5X SSC, 1X Denhardt's), then transferred through a wash Hybe dilution series into 2X SSC, then 0.2X SSC, and finally into MABT (100mM maleic acid, 150mM NaCl, 0.1% tween-20, pH7.5). Animals were blocked in MABT plus 1% BSA and 10% horse serum for one hour at room temperature (RT), and then labeled with a sheep anti-DIG antibody (1:2000, Roche) in MABT + BSA + 10% horse serum for four hours at RT. Animals were washed 8X with MABT and signal developed using NBT and BCIP. For *in situ* hybridizations on isolated cells, cells were fixed in 4% paraformaldehyde (PFA) in PBS for 20 min. at RT, treated with 1µg/mL proteinase K at RT for 10 min., and then post-fixed in 4% PFA for 15 min. at RT. Hybridization followed essentially the same protocol as described above.

Quantitative RT-PCR

RNA was extracted using the TriZol reagent (Invitrogen). Samples were DNase (Promega) treated at 37 °C x 15 min and then 70 °C x 15 min and cDNA was obtained from 1μg of total RNA by using SuperScript^{TM} II Reverse Transcriptase (Invitrogen). Clone H.55.12e (accession number: AY068123) was selected as an internal control as a constitutively expressed gene. Sets of specific *smedwi*-primers were used to evaluate gene expression. Samples without reverse transcriptase served as the negative control template. We used relative quantification to evaluate gene expression levels from control and γ-irradiated planarians, as well as from different cell populations. Total RNA from intact worms (2 μg) or from sorted cells (20 ng) was used to synthesize template cDNA. PCR reactions were performed using the SYBR® Green RT-PCR kit (Applied Biosystems) and reactions analyzed using an ABI Prism® 7900HT (Applied Biosystems). Reactions were run in triplicate and at least two different experiments per condition were performed. Relative standard curves for each experiment were created from H.55.12e data. Data were analyzed using SDS 2.1 software (Applied Biosystems).

RNAi

The cDNAs H.2.12C and HB.14.6D were used for the RNAi of *smedwi-1* and *smedwi-2*, respectively. RNAi, unless stated otherwise, involved two dsRNA feedings four days apart. dsRNA that was delivered by injections was prepared using T7 and T3 RNA polymerases, and 32nL was injected 3X on each of three days. RNAi by feeding utilized the pDONRdT7 vector and methods previously described (*1*).

FACS

Planarians were amputated into small pieces in cold calcium, magnesium-free medium (CMF plus BSA) containing Trypsin Inhibitor Type II-0 (30μg/mL) and then placed into CMF containing Trypsin (2 units/mL) and left to rock for 2 hours at 4°C. (CMF plus BSA; 15mM Hepes, 400mg/L NaH_2PO_4, 800mg/L NaCl, 1200mg/L KCl, 800mg/L $NaHCO_3$, 240mg/L glucose, 1% BSA, pH7.3). Cells were collected by centrifugation, resuspended in CMF+BSA, then passed through 53μm and 20μm Nitex filters sequentially. Cells were then collected by centrifugation and re-suspended in fresh CMF+BSA plus Hoechst33342 (7.5μg/mL) and Calcein (0.5μg/mL) and allowed to sit at RT for 20min. Cells were collected, resuspended in CMF+BSA and 5μg/mL propidium iodide was added. Analyses and sorts were performed using a Becton Dickinson FACSvantage.

BrdU labeling, antibody labeling, tissue sectioning, and microscopy

Animals were fed artificial planarian food containing 5mg/mL BrdU plus 0.6% ultra low gelling temperature agarose, 35% blended liver, and red food coloring to color. Animals were killed in 2% HCl for 30-60 seconds at RT, then fixed in Carnoy's fixative for 3 hours at RT. Animals were rinsed in methanol and then bleached overnight in 6% hydrogen peroxide in methanol. Animals were re-hydrated through a methanol dilution series in PBST (0.3% triton X-100) and then treated with 2N HCl at RT for 45 min. Followed by a rinse with 0.1M Borax in PBS, animals were rinsed 3X with PBST (0.3% triton X-100) then blocked at RT for 6h in PBST + 0.25% BSA. Animals were incubated

overnight in 1:10 rat anti-BrdU (Oxford Biotech), washed 7X over 6h the next day, incubated overnight in 1:100 goat anti-rat conjugated to HRP (AbCam), then labeled with tyramide conjugated to Alexa568 (Molecular Probes) as previously described (*1*). Whole-mount confocal microscopy was carried out on BrdU-labeled animals using an Olympus Fluoview confocal microscope. Animals were labeled with the anti-phosphorylated histone H3 antibody as described previously (*1*). Numbers of mitoses per length were determined by counting labeled cell nuclei and dividing the numbers by animal lengths in mm. For tissue sectioning, animals were incubated in 2% and then 10% Sucrose in PBST for 1 hour each, rocking at RT. Animals were then left to rock in 25% sucrose in PBST overnight at RT. Animals were embedded in OCT and 15μm sections created. Sections were observed using Nomarski optics.

Table S1. *smedwi* expression is greatly reduced by irradiation

	Expression relative to control	
Gene	**Wild-type animals**	**Irradiated (6K Rad) animals**
smedwi-1	18.8 ± 1.4	1.9e-06 ± 7.6e-08
smedwi-2	6.9 ± 0.14	0.3 ± 0.001

Results represent mean ± SD of three experiments. Data are relative to expression detected for the ubiquitously expressed control H.55.12e. See methods for details.

Table S2. *smedwi* genes are predominantly expressed in X1 cells

	Expression relative to control		
Gene	**Xins cells**	**X1 cells**	**X2 cells**
smedwi-1	0.01 ± 0.002	8,498 ± 4,341	48.5 ± 22.5
smedwi-2	0.5 ± 0.1	1,017 ± 516	24.9 ± 14.0

Results represent mean ± SD of three experiments. Data are relative to expression detected for the ubiquitously expressed control H.55.12e. See Fig. 1F for cell isolation details and nomenclature. See methods for details.

Fig. S1. SMEDWI-1 and –2 are homologous to the *Drosophila* proteins PIWI and AGO2. AGO2 is a representative of the Argonaute class and PIWI of the PIWI class of proteins. Top, PAZ domains. Bottom, PIWI domains. Amino acids (aa) labeled with a red circle beneath them indicate the putative RNase active site caboxylate residues (*2*). Yellow circles indicate candidate aa that create a binding pocket for the 5'-phosphate of RNA (*3*). Blue circles indicate aa that can distinguish between the Argonaute and PIWI classes (*4*). GeneBank accession numbers for *smedwi-1* and *smedwi-2* are DQ186985 and DQ186986.

Fig. S2. Supplemental results related to the RNAi of *smedwi-2*. **(A)** *smedwi-1(RNAi)* eliminates detectable *smedwi-1* message (animal is 13d post RNAi) and *smedwi-2(RNAi)* (animal is 8 days RNAi) eliminates detectable *smedwi-2* message. **(B)** Summary time course of the progression of the *smedwi-2(RNAi)* phenotype. See text for details. 7/7 animals cut eight days and 18/18 animals cut 10 days following *smedwi-2* dsRNA exposure failed to generate a blastema. Multiple other experiments corroborated these example results. **(C)** *smedwi-2(RNAi)* animals cut early after exposure to dsRNA regenerated small blastemas that regressed. (e.g., 8/8 animals cut four or six days following exposure to dsRNA.) Animals were injected dsRNA 3X32nl per day for three days and then amputated on the following day. Mock treated animals were injected with water. Animals were decapitated and had their tails removed; blastemas are unpigmented. White dotted line indicates amputation site. White arrows point to blastemas. Yellow arrows point to regressed blastemas. Anterior, left. Bar, 0.2mm. **(D)**

To determine whether the presence of neoblasts or the capacity to undergo mitosis was affected by *smedwi-2(RNAi)*, we first performed *in situ* hybridizations with the *smedwi-1* riboprobe. By 12 days following exposure to dsRNA 9/9 *smedwi-2(RNAi)* animals had qualitatively normal *smedwi-1* signal and by 15 days 9/9 *smedwi-2(RNAi)* animals had very low *smedwi-1* signal. Anterior, left. Bar, 0.2mm. d, days following first feeding of dsRNA. αH3P, anti-phosphorylated histone H3 antibody.

Fig. S3. X1 and X2 cell populations decline at late time points following exposure to *smedwi-2* dsRNA. Cell populations were analyzed by FACS. Though batch to batch variation in cell preparations make quantitative comparisons somewhat variable, trends are readily apparent. Cell populations were analyzed as described in the Figs. 1 and 2 legends. Y axis indicates the percentage of cells that were propidium iodide negative and Hoechst 33342 positive and were within the gates for X1 and X2 as defined in Fig. 2G. X axis indicates the number of days following the first of two dsRNA feedings of either *smedwi-2* dsRNA or control *unc-22* dsRNA.

Fig. S4. *smedwi-2(RNAi)* neoblast progeny cells that enter the epidermis are morphologically abnormal. Figure 3C displays an example at higher magnification of abnormal epidermal morphology. Post-pharyngeal cross-sections 13 days following RNAi and 6 days post-BrdU labeling. Black arrowheads, BrdU positive cells intercalating in epidermis (outer-most cells). Ventral surface, left. Bar, 100μm.

1. P. W. Reddien, A. L. Bermange, K. J. Murfitt, J. R. Jennings, A. Sánchez Alvarado, *Dev. Cell* **8**, 635 (2005).

2. J. J. Song, S. K. Smith, G. J. Hannon, L. Joshua-Tor, *Science* **305**, 1434 (2004).
3. J. B. Ma *et al.*, *Nature* **434**, 666 (2005).
4. J. S. Parker, S. M. Roe, D. Barford, *EMBO* **23**, 4727 (2004).

Figure S1

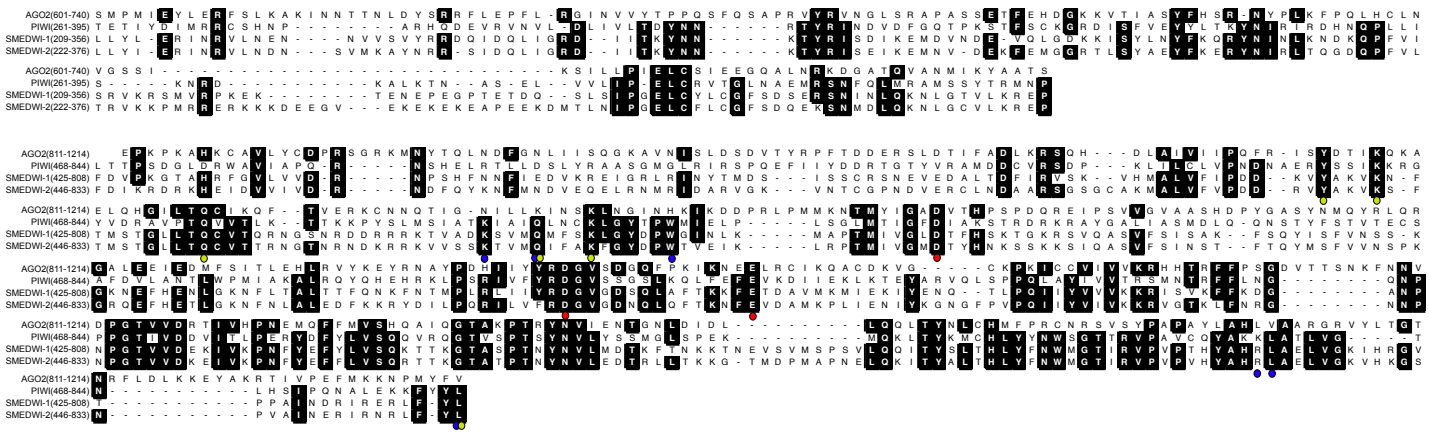
AGO2(601-740)
PIWI(261-395)
SMEDWI-1(209-356)
SMEDWI-2(222-376)
AGO2(811-1214)
PIWI(468-844)
SMEDWI-1(425-808)
SMEDWI-2(446-833)

Figure S2

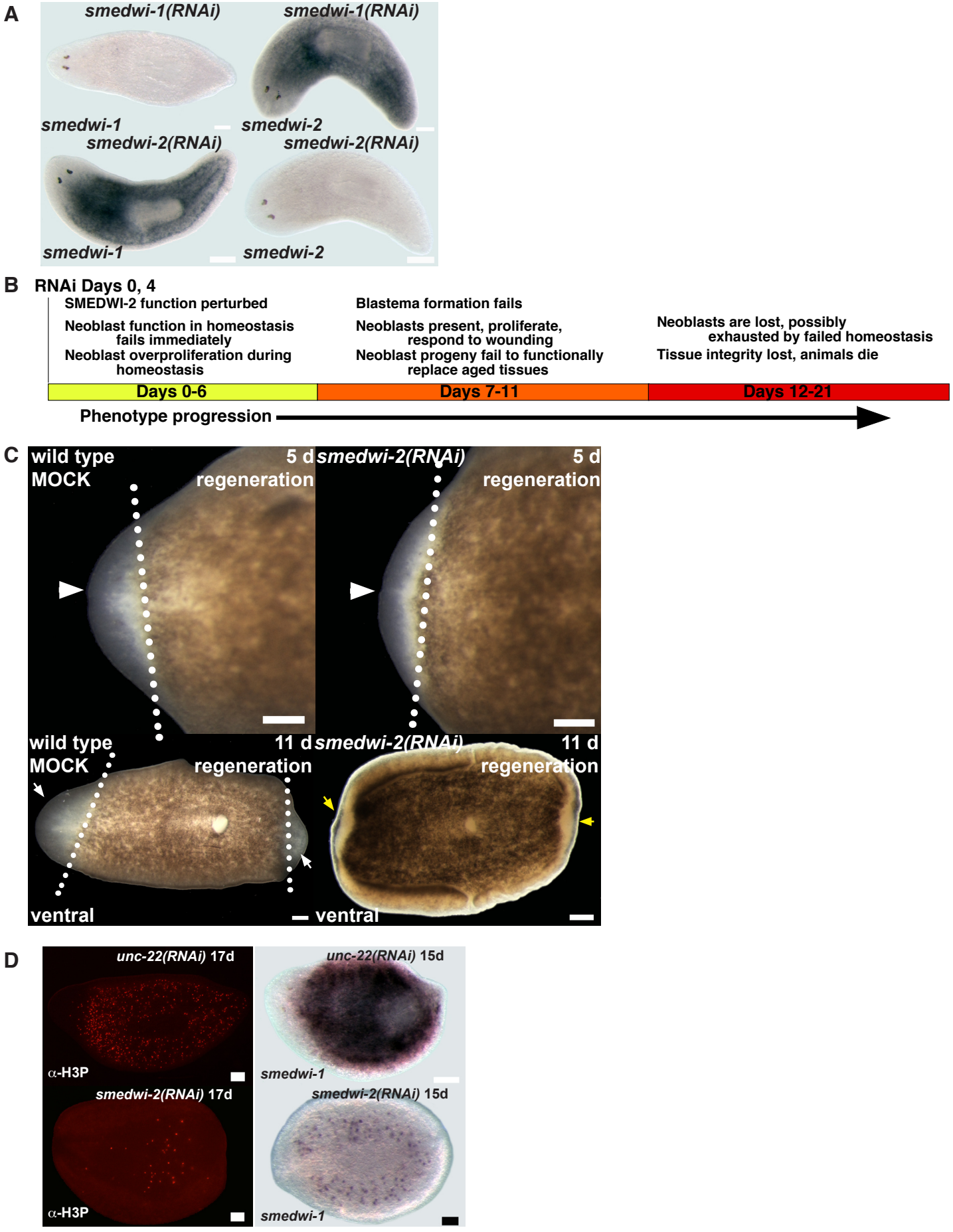
A
smedwi-1(RNAi)
smedwi-1(RNAi)
smedwi-1
smedwi-2
smedwi-2(RNAi)
smedwi-2(RNAi)
smedwi-1
smedwi-2
B
RNAi Days 0, 4
SMEDWI-2 function perturbed
Neoblast function in homeostasis fails immediately
Neoblast overproliferation during homeostasis
Blastema formation fails
Neoblasts present, proliferate, respond to wounding
Neoblast progeny fail to functionally replace aged tissues
Neoblasts are lost, possibly exhausted by failed homeostasis
Tissue integrity lost, animals die
Days 0-6
Days 7-11
Days 12-21
Phenotype progression
C
wild type MOCK
5 d regeneration
smedwi-2(RNAi)
5 d regeneration
wild type MOCK
11 d regeneration
smedwi-2(RNAi)
11 d regeneration
ventral
ventral
D
unc-22(RNAi) 17d
α-H3P
smedwi-2(RNAi) 17d
α-H3P
unc-22(RNAi) 15d
smedwi-1
smedwi-2(RNAi) 15d
smedwi-1

Figure S3

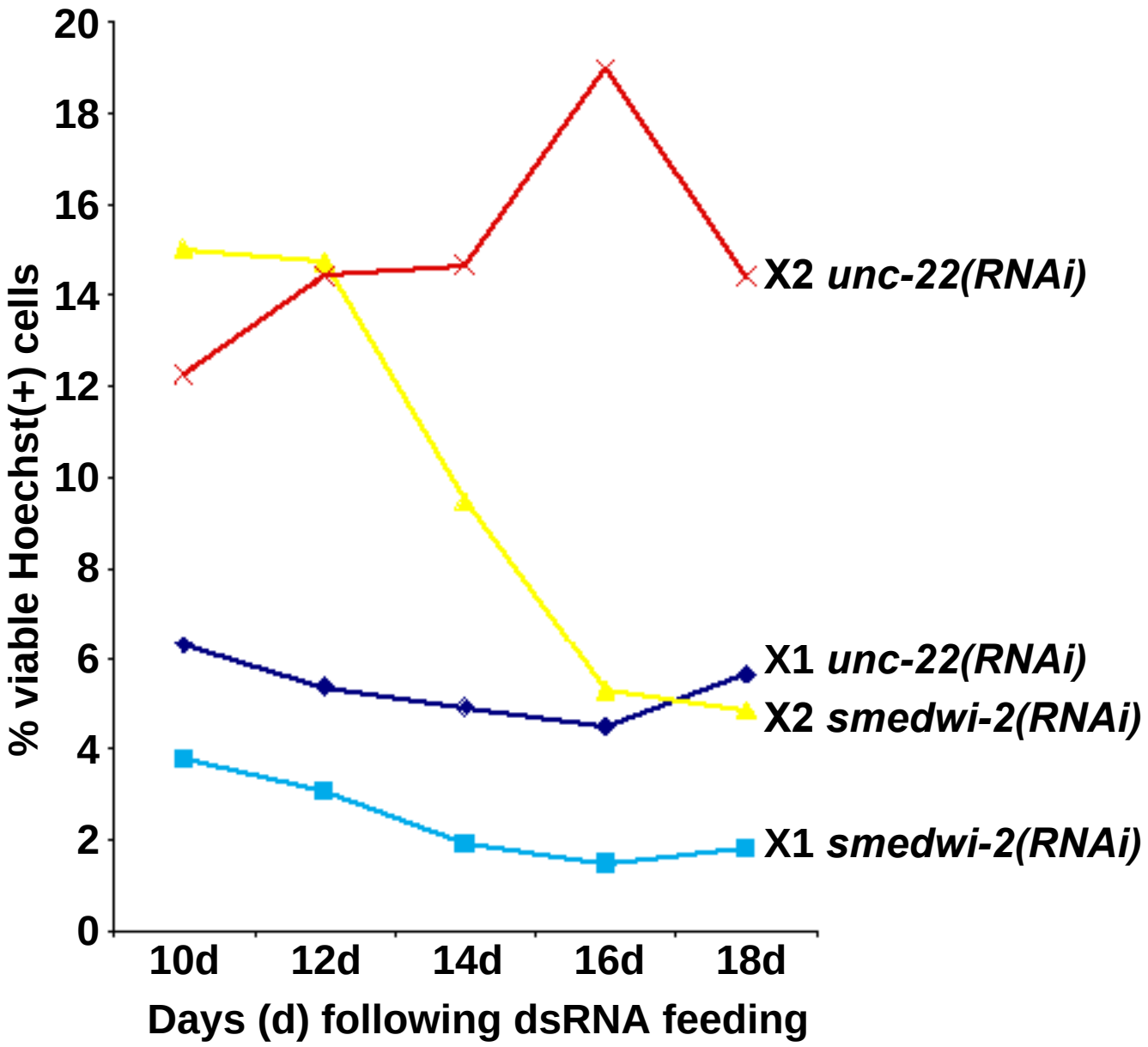
20
18
16
14
12
10
8
6
4
2
0
% viable Hoechst(+) cells
10d
12d
14d
16d
18d
Days (d) following dsRNA feeding
X2 unc-22(RNAi)
X1 unc-22(RNAi)
X2 smedwi-2(RNAi)
X1 smedwi-2(RNAi)

Figure S4

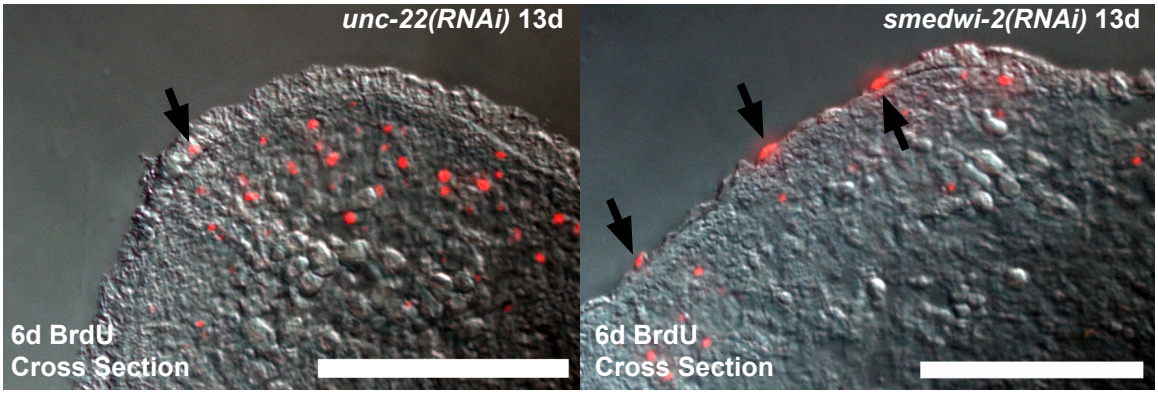
unc-22(RNAi) 13d
6d BrdU
Cross Section
smedwi-2(RNAi) 13d
6d BrdU
Cross Section